MOLECULAR AND CELLULAR BIOLOGY, July 1997, p. 4070–4079 Vol. 17, No. 7
0270-7306/97/$04.00+0

DNA Cleavage within the *MLL* Breakpoint Cluster Region Is a Specific Event Which Occurs as Part of Higher-Order Chromatin Fragmentation during the Initial Stages of Apoptosis

MARTIN STANULLA,[1,2,3] JUNJIE WANG,[1,4] DAVID S. CHERVINSKY,[1,2] SRINIVAS THANDLA,[2,5] AND PETER D. APLAN[1,2,5]*

Departments of Molecular Medicine[1] Pediatrics,[2] and Biochemistry,[4] Roswell Park Cancer Institute, Buffalo, New York 14263; Children's Hospital of Buffalo, Buffalo, New York, 14222[5]; and Department of Pediatric Hematology/Oncology, Hannover Medical School, Hannover, Germany[3]

Received 24 December 1996/Returned for modification 5 February 1997/Accepted 2 April 1997

A distinct population of therapy-related acute myeloid leukemia (t-AML) is strongly associated with prior administration of topoisomerase II (topo II) inhibitors. These t-AMLs display distinct cytogenetic alterations, most often disrupting the *MLL* gene on chromosome 11q23 within a breakpoint cluster region (bcr) of 8.3 kb. We recently identified a unique site within the *MLL* bcr that is highly susceptible to DNA double-strand cleavage by classic topo II inhibitors (e.g., etoposide and doxorubicin). Here, we report that site-specific cleavage within the *MLL* bcr can be induced by either catalytic topo II inhibitors, genotoxic chemotherapeutic agents which do not target topo II, or nongenotoxic stimuli of apoptotic cell death, suggesting that this site-specific cleavage is part of a generalized cellular response to an apoptotic stimulus. We also show that site-specific cleavage within the *MLL* bcr can be linked to the higher-order chromatin fragmentation that occurs during the initial stages of apoptosis, possibly through cleavage of DNA loops at their anchorage sites to the nuclear matrix. In addition, we show that site-specific cleavage is conserved between species, as specific DNA cleavage can also be demonstrated within the murine *MLL* locus. Lastly, site-specific cleavage during apoptosis can also be identified at the *AML1* locus, a locus which is also frequently involved in chromosomal rearrangements present in t-AML patients. In conclusion, these results suggest the potential involvement of higher-order chromatin fragmentation which occurs as a part of a generalized apoptotic response in a mechanism leading to chromosomal translocation of the *MLL* and *AML1* genes and subsequent t-AML.

Nonrandom chromosomal aberrations, particularly chromosomal translocations, are frequently found in association with a wide spectrum of malignancies, most prominently leukemias and lymphomas (9, 14, 47). The available evidence suggests that these nonrandom chromosomal translocations are often causal events leading to malignant transformation (2, 40). However, the molecular mechanisms which cause these translocations remain largely unknown.

In many cases, a powerful argument can be made that these translocations are the result of mistakes in normal V(D)J recombinase activity (4, 60). These arguments are based on identification of features that resemble normal V(D)J recombinase activity, such as cryptic heptamer sequences, nontemplated N-region nucleotide addition, and exonucleolytic deletion of germ line nucleotides at the translocation breakpoints (4, 60). Other factors that have been implicated in the generation of nonrandom translocations include homologous recombination events between *Alu* elements (52) and exposure to DNA-damaging agents (35, 36). It has been recognized for some time that DNA-damaging cancer chemotherapeutic agents, such as the topoisomerase II (topo II) inhibitor etoposide (36) and the alkylating agent melphalan (35), can cause chromosomal translocations. For instance, phytohemagglutinin-stimulated peripheral blood lymphocytes treated in vitro with etoposide and allowed to recover for 24 h prior to karyotypic analysis demonstrate numerous structural chromosomal abnormalities, including translocations, inversions, and dicentric chromosome formation (36). Although no chromosomal region was spared from the abnormalities caused by etoposide treatment, certain hot spots were recurrently involved, suggesting the existence of chromosomal sites that were susceptible to recombination induced by etoposide. One plausible interpretation of these studies is that the etoposide-treated lymphocytes have repaired DNA damage caused by etoposide improperly, with two distinct chromosomes becoming joined together during the repair process, resulting in a chromosomal translocation.

An additional line of investigation supporting the contention that topo II inhibitors can cause chromosomal translocations comes from the study of patients with therapy-related acute myelogenous leukemia (t-AML) following treatment of a primary malignancy with topo II inhibitors (20, 24, 44, 48, 53). Patients with t-AML associated with antecedent topo II inhibitor therapy generally display distinct clinical and biological features. The t-AML characteristically occurs within 36 months of treatment, is not usually associated with a preceding myelodysplastic syndrome, often displays a monocytic phenotype, and typically demonstrates cytogenetic abnormalities at chromosome 11q23 or, less frequently, 21q22 (44, 45, 53). The *MLL* gene (also known as *ALL-1* or *HRX*) is almost always disrupted by the 11q23 breakpoints, which generally occur within an 8.3-kb breakpoint cluster region (bcr) (20, 24, 59). It

* Corresponding author. Mailing address: Department of Pediatrics, Roswell Park Cancer Institute, Buffalo, NY 14263. Phone: (716) 845-4598 or (716) 845-5773. Fax: (716) 845-4502. E-mail: paplan@sc3101.med.buffalo.edu.

has been proposed that topo II inhibitors induce chromosomal breakage within the *MLL* gene, with *MLL* translocations resulting from mistakes in the DNA repair process (53, 57). The resultant *MLL* fusion proteins produced by the translocations are thought to be causal factors in the development of these leukemias (50). The clinical relevance of t-AML is underscored by the results of a recent clinical trial employing multiagent chemotherapy, including the epipodophyllotoxin etoposide, as the initial therapy for childhood B-cell precursor acute lymphoblastic leukemia. In that trial, more children developed t-AML than suffered a relapse of their primary leukemia (62).

While the specific events by which topo II inhibitors cause chromosomal translocations remain largely uncharacterized, a recent study has demonstrated that *MLL* breakpoints in t-AML patients cluster within a high-affinity scaffold attachment region (SAR) (57). Eukaryotic DNA is organized in structural units, designated chromatin loops, that typically contain 50 to 100 kb of DNA. At their bases, these loops are anchored to a structure named the nuclear matrix or scaffold, which is the fraction of proteins retained in chromatin after depletion of most histone proteins by salt or nonionic detergent extraction (8, 38). The DNA sequences associated with the nuclear scaffold, the so-called matrix or SAR, are defined by their retention on the scaffold protein fraction after removal of bulk DNA or by their binding to isolated nuclear scaffolds in vitro (15, 23). When the *MLL* bcr was divided into centromeric and telomeric halves, 75% of the de novo leukemia breakpoints mapped to the centromeric half, while 75% of t-AML breakpoints were found in the telomeric half, which contains a high-affinity SAR (57). These results suggest that the events which lead to *MLL* translocations in t-AML patients may be distinct from those that cause *MLL* translocations in de novo AML patients. Intriguingly, an SAR within the murine immunoglobulin κ locus has been shown to be a preferred topo II cleavage site that occurs within 14 bp of a chromosomal translocation breakpoint, suggesting that illegitimate recombination events may be associated with both topo II and SARs (54).

Recently, we identified a unique site within the *MLL* bcr that is highly sensitive to double-strand DNA cleavage induced by topo II inhibitors and suggested that this site-specific cleavage may represent an initial step leading to *MLL* translocation and t-AML (5). This cleavage site was noted to colocalize with a consensus in vitro topo II recognition sequence (5′-GAGGA CCAGCTGGAAAAT-3′) (5, 55). In subsequent studies, we have begun a more detailed examination of *MLL* site-specific cleavage, focused on determining whether site-specific cleavage was more likely to be a direct effect of treatment with topo II inhibitors or a downstream effect of the genotoxic damage caused by these drugs. We report here that site-specific cleavage within the *MLL* bcr can be linked to the higher-order DNA fragmentation which occurs during the initial stages of apoptosis, suggesting a potential role for this type of chromatin fragmentation in the generation of chromosomal translocations.

MATERIALS AND METHODS

Cell lines, cell culture, and preparation of PBMC. The cell lines used in this study were MOLT-4 and CEM (both human T-cell leukemia), ML-1 and KG-1 (both human myeloid leukemia), 5637 (human bladder carcinoma), H69 (human small cell lung cancer), LBRM-33 (murine T-cell leukemia), and F4-6 (murine erythroleukemia). A list of references describing these cell lines is available upon request. In addition, a subset of experiments was performed with the topo II inhibitor-resistant cell line CEM/VM-1-5 and its parental CEM cell line (kind gift of William T. Beck) (17). Cell culture was performed by using RPMI 1640 supplemented with 10% fetal bovine serum, L-glutamine (2 mM), penicillin (100 U/ml), and streptomycin (100 μg/ml) (all from GIBCO, Grand Island, N.Y.). Peripheral blood mononuclear cells (PBMC) were isolated from peripheral blood of healthy normal individuals by Ficoll-Hypaque density centrifugation.

Treatment of cell lines and PBMC. After two washes with RPMI 1640, exponential-growth-phase cell lines or PBMC were resuspended at a density of 5×10^5 cells/ml in RPMI 1640 supplemented with 10% fetal bovine serum and incubated for 16 h with the indicated drug or vehicle alone, followed by isolation of genomic DNA for analysis. Cells were treated with either etoposide (10 or 30 μM), aclarubicin (0.1 μM), bimolane (20 μM), merbarone (10 μM), cytosine arabinoside (1, 3, or 6 μg/ml), methotrexate (10 μg/ml), *N*-methylformamide (300 mM), C_2 ceramide (25 μM), tumor necrosis factor alpha (TNF-α; 10 nM), sodium azide (300 mM), or dimethyl sulfoxide (DMSO; 30%) for 16 h. All agents were purchased from Sigma (St. Louis, Mo.) except bimolane and merbarone, which were obtained from Zenyaku Kogyo (Tokyo, Japan) and the NCI Drug Synthesis and Chemistry Branch (Bethesda, Md.), respectively. The agents were dissolved in either DMSO (etoposide, bimolane, and C_2 ceramide), sterile water (aclarubicin, merbarone, cytosine arabinoside, and sodium azide), 0.01 M sodium hydroxide (methotrexate), or phosphate-buffered saline (PBS; pH 7.4) supplemented with 0.1% bovine serum albumin (TNF-α). Serum starvation was performed by washing cells twice under serum-free conditions, resuspending exponential-growth-phase cells at a density of 5×10^5/ml in serum-free RPMI 1640, and incubating the cells for 56 h under standard cell culture conditions. Cell survival was estimated by trypan blue staining and subsequent exclusion of stained cells in a hemocytometer; genomic DNA was harvested for subsequent analysis as described previously (5).

Chromatin staining and nuclear fragmentation assay. The assay was modified from the one described by Oberhammer et al. (42). Treatment of cells was for 16 h with the exception of serum withdrawal, which was for 56 h. For some experiments, shorter (5-h) incubations were performed with 300 mM sodium azide and 30% DMSO in order to recover cells for morphologic analysis. Immediately after treatment, cells were centrifuged onto glass slides in a cytospin centrifuge, air dried, fixed for 30 min with 4% paraformaldehyde in PBS (pH 7.4) at room temperature, washed in PBS (pH 7.4), incubated for 2 min in permeabilization solution (0.1% Triton X-100, 0.1% sodium citrate) at 4°C, washed in PBS (pH 7.1), and stained with 8 μg of bisbenzimide (Hoechst 33258; Sigma) per ml in PBS (pH 7.1) for 15 min. Samples were then washed in PBS, mounted, coverslipped, and analyzed by fluorescence microscopy using a Nikon Optiphot microscope with a UV-2A filter (Nikon Inc., Melville, N.Y.). Fluorescent nuclei were scored and categorized according to their fragmentation status. Nuclei displaying ≥3 chromatin fragments were scored apoptotic; nuclei with <3 fragments were scored nonapoptotic. Two hundred nuclei were scored per sample.

In vitro DNA cleavage assay. An 8.3-kb genomic *Bam*HI fragment encompassing the *MLL* bcr was isolated from a human placental phage library (Stratagene, La Jolla, Calif.) by using standard techniques (51) and subsequently cloned into pBluescript II (Stratagene). Fifty nanograms of this plasmid linearized with *Not*I, or the same amount of gel-purified 8.3-kb *Bam*HI fragment, was incubated with 10 U of purified human topo IIα (Topogen, Columbus, Ohio) in a total volume of 20 μl, using the supplied buffer. Etoposide was added at the concentrations indicated in Fig. 1. Samples were incubated at 37°C for 30 min, followed by addition of sodium dodecyl sulfate and proteinase K (Gibco) to final concentrations of 0.1% and 0.1 mg/ml, respectively, and a second incubation at 42°C for 30 min. After ethanol precipitation, the samples were analyzed by indirect end labeling using the 0.2HB *MLL* cDNA probe or a 0.37-kb *Pvu*II-*Bam*HI genomic fragment, as described below.

Preparation and analysis of DNA. Genomic DNA was isolated by using a salting-out extraction procedure as previously described (5). Ten micrograms of genomic DNA was digested with the indicated restriction enzyme (Bethesda Research Laboratories, Gaithersburg, Md.), size fractionated on 0.8% agarose gels containing 1.0 μg of ethidium bromide per ml, photographed, denatured, neutralized, and transferred to nitrocellulose membranes (Schleicher & Schuell, Keene, N.H.). DNA was immobilized by UV cross-linking. A modification of the previously described indirect end-labeling (41) protocol was used to identify cleavage sites within the *MLL* locus, using a 0.2-kb *Hha*I-*Bam*HI cDNA fragment which included exons 9 to 11 (probe 0.2HB; nucleotides 4207 to 4423 of GenBank accession no. L04731), a 0.7-kb *MLL* cDNA fragment encompassing exons 5 to 7 and 9 to 11 (probe 0.7B from reference 37), and a 0.37-kb *Pvu*II-*Bam*HI genomic fragment encompassing the region from exons 10 to 11 (nucleotides 7969 to 8337 of GenBank accession no. U04737). The *AML1* probe C6E6H2 was a 0.24-kb *Hin*dIII-*Eco*RI cDNA fragment including exon 5 and 6 sequences (39). The mitochondrial DNA probe was a genomic fragment containing sequences from the mitochondrial gene encoding 16S RNA (3). Probes were labeled with ^{32}P by the random-priming technique, using a Prime-It II kit (Stratagene) according to the manufacturer's protocol, and hybridized to Southern blots as previously described (5, 18). Final washing conditions were 0.1% sodium dodecyl sulfate–0.1× SSC (1× SSC is 0.15 M NaCl plus 0.015 M sodium citrate) at 52°C for all probes. Autoradiography of blots was performed for 1 to 5 days at −70°C with an intensifying screen. Analysis of oligonucleosomal DNA fragmentation was performed by conventional gel electrophoresis using 2% agarose gels containing 1.0 μg of ethidium bromide per ml. The gels were visualized with a UV transilluminator, and pictures were taken with a gel documentation and analysis system (Alpha Innotech Corporation, San Leandro, Calif.).

FIGE. Field inversion gel electrophoresis (FIGE) was carried out as described previously (7, 43), with minor modifications. A total of 5×10^6 cells were harvested either before or at timed intervals after etoposide or *N*-methylform-

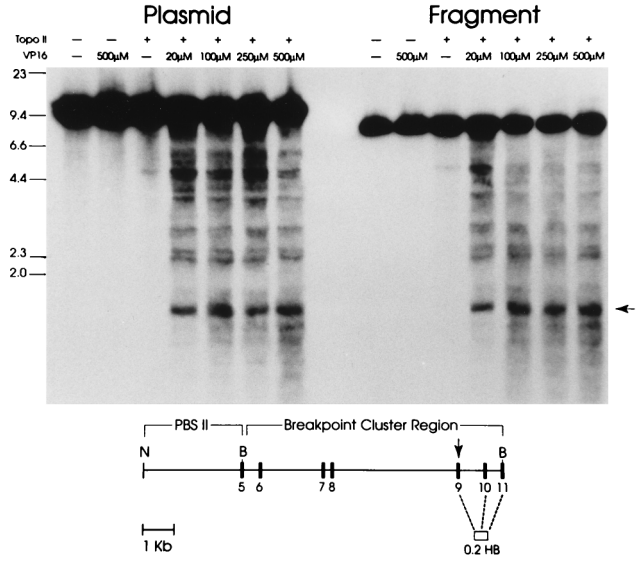

FIG. 1. DNA cleavage induced by the topo II inhibitor etoposide in vitro. Fifty nanograms of either an 8.3-kb genomic fragment encompassing the *MLL* bcr (right) or a plasmid containing this fragment, linearized with *Not*I (left), was incubated with 10 U of topo II and etoposide as indicated. The samples were analyzed by indirect end labeling using the 0.2HB *MLL* cDNA probe, which contains exon 9, 10, and 11 sequences. The most prominent etoposide-induced band, indicated by an arrow on the right, is the same size as the fragment produced in vivo. Size standards are indicated in kilobases. The map displays the plasmid containing the 8.3-kb *MLL* bcr. Exons are shown as solid boxes; restriction sites for *Bam*HI (B) and *Not*I (N) are indicated; PBS II stands for pBluescript II. The location of the previously identified (5) etoposide-induced in vivo cleavage site is indicated by an arrow.

amide treatment and embedded in 0.1 ml of a 1% Incert (FMC, Rockland, Maine) agarose solution. Proteins were digested by a 24-h incubation with proteinase K (1 mg/ml), and the agarose plugs were washed four times with a 20 mM Tris (pH 8.0)–50 mM EDTA solution prior to FIGE. Genomic DNA fragments were separated by FIGE using 1.5% agarose (Bio-Rad, Hercules, Calif.) gels in an H4 (Bethesda Research Laboratories) electrophoresis chamber with 0.25× TAE (1× TAE is 40 mM Tris, 40 mM acetate, and 2 mM EDTA [pH 8.5]). Gels were run with recirculation in a cold room at 4°C, using a FIGE Mapper system (Bio-Rad). The forward vector (150V) had an initial switch time of 0.5 s and a final switch time of 10 s. The reverse vector (150V) had an initial switch time of 0.2 s and a final switch time of 3.3 s (constant forward/reverse ratio of 3:1). This program was run for 20 h, followed immediately by a second program with 150V vectors, also run for 20 h: forward vector initial switch time of 10 s and final switch time of 60 s; reverse vector initial switch time of 3.3 s and final switch time of 20 s (constant forward/reverse ratio of 3:1).

RESULTS

In vitro cleavage of the *MLL* bcr by topo II. We have previously demonstrated that site-specific cleavage within the *MLL* bcr can be induced by topo II inhibitor treatment of intact cells (reference 5; also see Fig. 2). To determine whether a similar pattern of site-specific cleavage within the *MLL* bcr could be induced by topo II inhibitors in assays using naked DNA and a cell-free system, we treated a cloned genomic DNA fragment encompassing the *MLL* bcr with etoposide and purified human topo II. DNA cleavage was assayed by an indirect end-labeling strategy using the 0.2HB *MLL* cDNA probe (Fig. 1). A similar pattern of cleavage was observed with either an isolated fragment or a linearized plasmid containing the fragment. In addition, a similar cleavage pattern was observed with a 0.37-kb *Pvu*II-*Bam*HI genomic *MLL* probe from the 3′ end of the *MLL* bcr (data not shown). In contrast to the DNA cleavage pattern induced by topo II inhibitor treatment of intact cells (5), multiple cleavage sites were detectable in this in vitro assay. However, at all etoposide concentrations used in our in vitro assay system, one of the most prominent bands produced in vitro was 1.6 kb, which comigrated with the fragment produced by the treatment of intact cells with topo II inhibitors (Fig. 2).

In vivo site-specific cleavage within the *MLL* bcr can be induced by catalytic topo II inhibitors. To further investigate the role of topo II during induction of site-specific cleavage within the MLL bcr, we treated MOLT-4 cells with the catalytic topo II inhibitors aclarubicin, bimolane, and merbarone. Whereas classic or noncatalytic topo II inhibitors such as the epipodophyllotoxin etoposide or the anthracycline doxorubicin damage DNA by stabilizing topo II intermediates covalently bound to the phosphodiester backbone (the cleavable complex), catalytic topo II inhibitors interact with topo II prior to its binding DNA and therefore inhibit the formation of cleavable complexes (12). Unexpectedly, the catalytic topo II inhibitors produced the same cleavage pattern in MOLT-4 cells as did the classic topo II inhibitors (Fig. 2B; the *MLL* bcr map is shown in Fig. 2A). Moreover, additional control experiments using either antimetabolite (methotrexate) or nucleoside analog (cytosine arabinoside) chemotherapeutic agents generated a pattern of site-specific *MLL* cleavage which was indistinguishable from that generated by etoposide (Fig. 2C), although neither of these agents is known to be a topo II inhibitor. Taken together, these findings suggested that cleavable complex formation may not be a prerequisite for *MLL* site-specific cleavage.

To further investigate the surprising finding that site-specific *MLL* cleavage could be induced by catalytic topo II inhibitors as well as chemotherapeutic agents not targeting topo II, we treated a cell line which is resistant to the classic topo II inhibitor etoposide with either etoposide or the nucleoside analog cytosine arabinoside, which acts by chain termination during DNA replication (26). The cell line used for this experiment, CEM/VM-1-5, is 140 times more resistant to the cytotoxic effects of the epipodophyllotoxin teniposide than the parental CEM cell line (17). The resistance of this cell line has been attributed to point mutations involving the genes coding for both topo IIα and topo IIβ, resulting in reduced formation of cleavable complexes, less DNA damage, and less cytotoxicity (6, 12, 17, 21). We treated parental CEM and CEM/VM-1-5 cells with 10 μM etoposide or 6 μg of cytosine arabinoside per ml for 16 h and assessed the presence of site-specific cleavage by indirect end labeling (Fig. 2D). Both etoposide and cytosine arabinoside induced site-specific cleavage within the *MLL* bcr of the parental CEM cells, whereas the CEM/VM-1-5 cell line was resistant to site-specific cleavage induced by etoposide. In contrast, site-specific cleavages induced by cytosine arabinoside were similar in the parental CEM cell line and the etoposide-resistant CEM/VM-1-5 cell line. Thus, we inferred that site-specific cleavage within the *MLL* bcr could be produced by a downstream event common to cytosine arabinoside and etoposide and was not necessarily a direct effect of etoposide, such as cleavable complex formation.

Site-specific *MLL* bcr cleavage can be induced by apoptosis. A reasonable candidate for a downstream event which might cause site-specific DNA cleavage within the *MLL* bcr is programmed cell death or apoptosis. Apoptosis is a genetically conserved program involving cytoplasmic and nuclear events leading to cell shrinkage, chromatin condensation, and internucleosomal DNA fragmentation (10, 22, 61, 63). The distinct morphologic changes as well as internucleosomal DNA fragmentation are characteristics of apoptosis which are often used to distinguish apoptotic cell death from necrotic cell death initiated through physical injury (61, 63). Apoptosis can be triggered by a wide spectrum of agents, including DNA-dam-

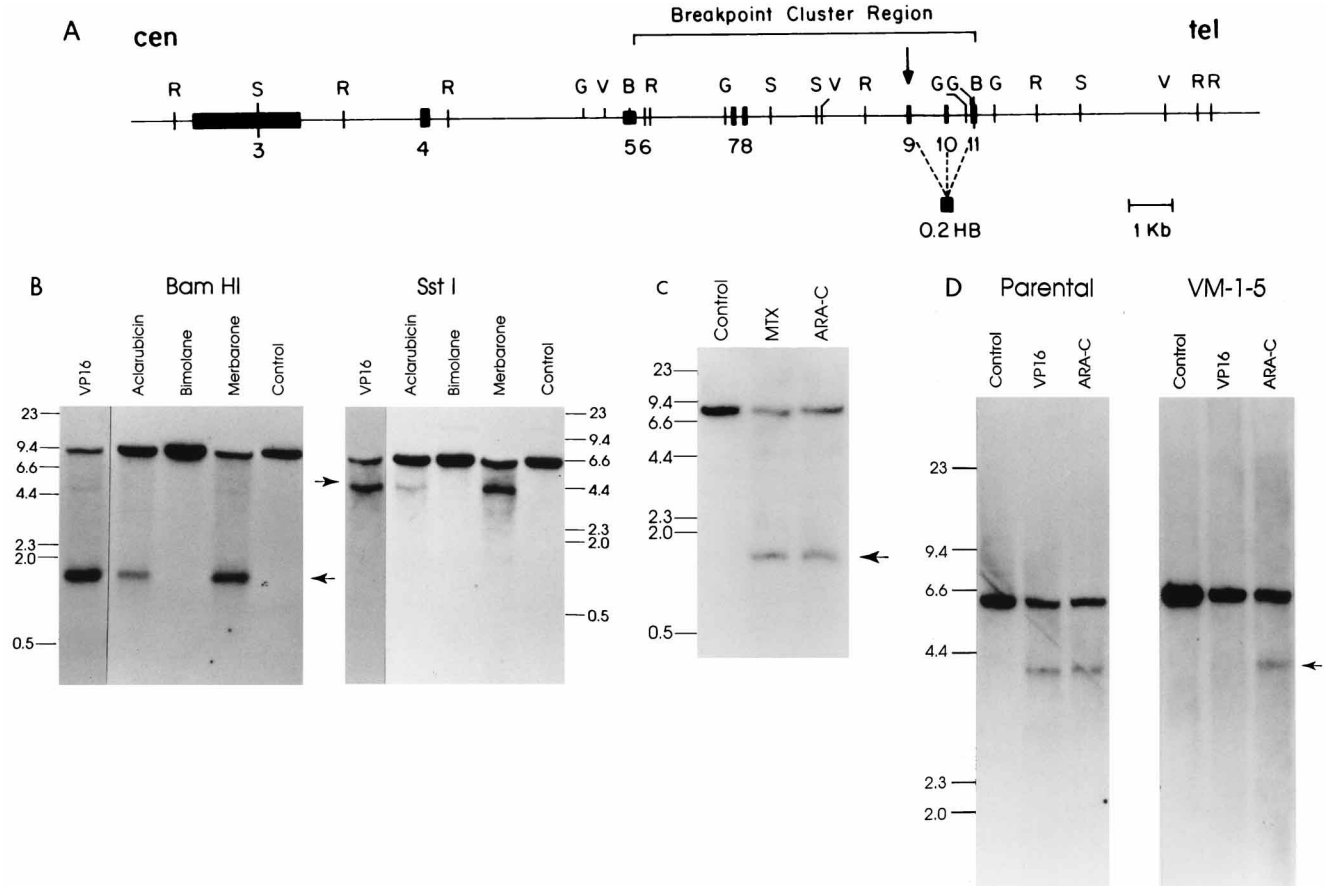

FIG. 2. (A) *MLL* restriction map. The bcr is bracketed; exons are shown as solid boxes. Chromosomal orientation from centromere (cen) to telomere (tel) is as indicated. The point of site-specific cleavage is indicated by an arrow. The cDNA probe 0.2HB includes exon 9, 10, and 11 sequences as indicated. Restriction enzyme sites (not complete outside of the bcr): R, *Eco*RI; S, *Sst*I; G, *Bgl*II; V, *Eco*RV; B, *Bam*HI. (B) Site-specific cleavage within the *MLL* bcr induced by etoposide and catalytic topo II inhibitors. MOLT-4 cells were treated for 16 h with either 10 μM etoposide (VP16), vehicle alone (Control; 0.01% DMSO), 0.1 μM aclarubicin, 20 μM bimolane, or 10 μM merbarone. Genomic DNA was digested with either *Bam*HI or *Sst*I, size fractionated on agarose gels, transferred to nitrocellulose membranes, and analyzed by indirect end labeling using the 0.2HB *MLL* cDNA probe. Drug-induced bands are indicated by an arrow; size standards are in kilobases. A faint band in the bimolane lane is seen on prolonged exposure of the autoradiograph. (C) Site-specific *MLL* bcr cleavage induced by treatment of MOLT-4 cells with either vehicle alone (Control; 10 μM sodium hydroxide), 1 μg of cytosine arabinoside (ARA-C) per ml, or 10 μg of methotrexate (MTX) per ml for 16 h. Analysis was performed with *Bam*HI-digested genomic DNA by indirect end labeling using the 0.2HB *MLL* cDNA probe. Drug-induced bands are indicated by an arrow; size standards are in kilobases. (D) Site-specific cleavage within the *MLL* bcr of the etoposide-resistant cell line CEM/VM-1-5 and its parental CEM cell line. Cells were treated with either vehicle alone (Control; 0.01% DMSO), 10 μM etoposide (VP16), or 6 μg of cytosine arabinoside (ARA-C) per ml for 16 h. Genomic DNA was digested with *Sst*I and analyzed by indirect end labeling with the 0.2HB *MLL* cDNA probe. Drug-induced bands are indicated by an arrow; size standards are in kilobases.

aging chemotherapeutic agents such as etoposide, cytosine arabinoside, and methotrexate (26, 31), as well as nongenotoxic compounds and biological stimuli, such as TNF-α (34) or Apo-1/Fas (13, 61).

To test the hypothesis that site-specific cleavage within the *MLL* bcr is part of a general apoptotic program, we treated MOLT-4 cells with stimuli that induce either apoptotic or necrotic cell death. Genomic DNA was assayed for site-specific *MLL* bcr cleavage by indirect end labeling. As inducers of apoptosis, both genotoxic stimuli (etoposide and cytosine arabinoside) (26, 31) and nongenotoxic stimuli such as *N*-methylformamide (7), C_2 ceramide (13), TNF-α (34), or serum starvation were used (33, 43). Necrotic cell death was brought about by exposure of cells to 30% DMSO (58) or 300 mM sodium azide (27). For apoptosis verification, the mode of cell death was assessed through analysis of morphologic changes by staining with the DNA-specific fluorochrome bisbenzimide (Hoechst 33258) (42). Figure 3A indicates that characteristic features of apoptosis could be observed when cells were exposed to apoptotic stimuli but not in cells treated with stimuli that induced necrotic cell death. Estimates of cell survival and the proportion of apoptotic cells by trypan blue staining and nuclear fragmentation assay, respectively, are shown in Table 1.

Genomic DNA isolated from these experiments was analyzed for evidence of *MLL* site-specific cleavage by indirect end labeling using the 0.2HB *MLL* cDNA probe. Figure 3B demonstrates that site-specific cleavage within the *MLL* bcr correlated with apoptosis, as it was detectable in all of the apoptotic DNA samples but not in the control sample or in the necrotic DNA samples. As can be seen in Fig. 3B, the degree of site-specific cleavage varied with the stimuli used to induce apoptosis; site-specific cleavage was most evident with etoposide while only faintly evident with TNF-α. In general, the degree of site-specific cleavage correlated with the degree of apoptosis as estimated by the nuclear fragmentation assay (Fig. 3B; Table 1). We also compared the degree of oligonucleosomal DNA fragmentation with site-specific cleavage (Fig. 3B and C). Although MOLT-4 cells have been reported to not demonstrate oligonucleosomal DNA fragmentation during apoptosis (11),

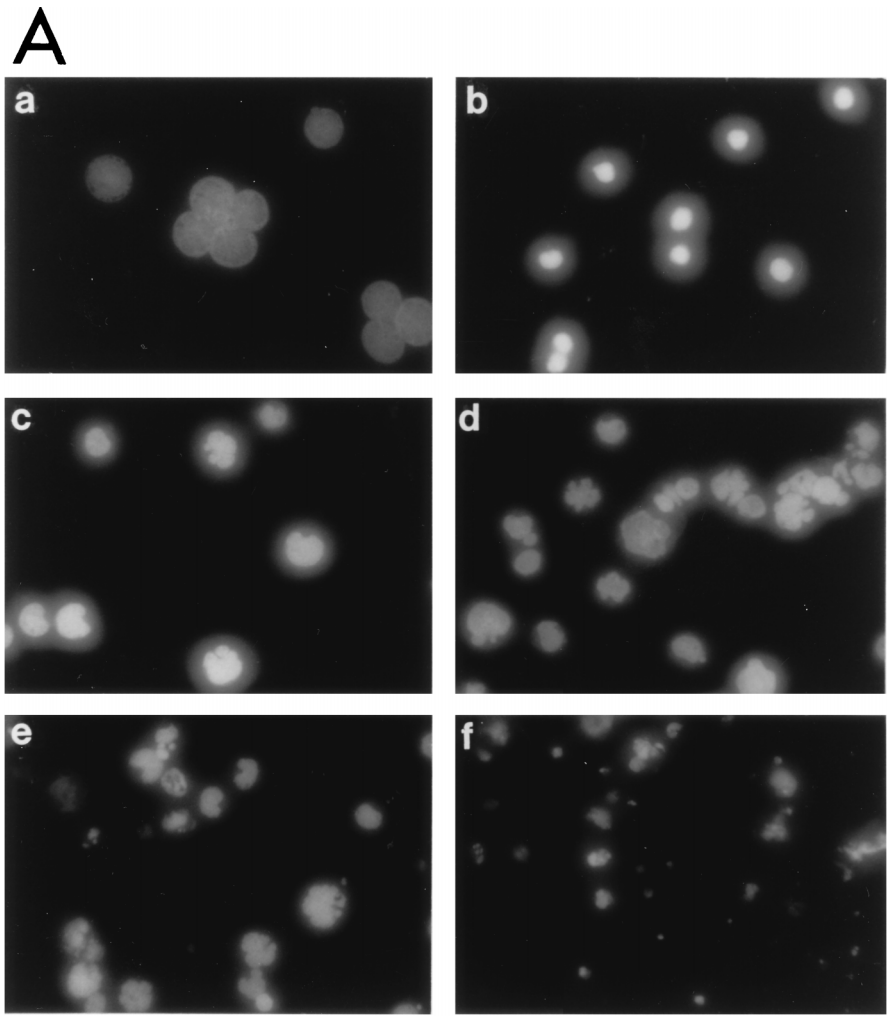

FIG. 3. (A) Morphological features of MOLT-4 nuclei stained with the DNA-specific fluorochrome Hoechst 33258. a, Untreated control; b, 30% DMSO for 5 h; c, 300 mM *N*-methylformamide for 8 h; d, 300 mM *N*-methylformamide for 16 h; e, 30 μM etoposide for 8 h; f, 30 μM etoposide for 16 h. Note the nuclear fragmentation induced by *N*-methylformamide and etoposide but not by DMSO. (B) Site-specific cleavage within the *MLL* bcr induced by various apoptotic stimuli but not by necrotic stimuli. MOLT-4 cells were either treated for 16 h with vehicle alone (Control; 0.03% DMSO), 300 mM sodium azide (NaN_3), 30% DMSO, 30 μM etoposide (VP16), 3 μg of cytosine arabinoside (ARA-C) per ml, 300 mM *N*-methylformamide (NMF), 25 μM C_2 ceramide, and 10 nM TNF-α or subjected to 56 h of serum withdrawal (Starved). Genomic DNA was analyzed by indirect end labeling using the 0.2HB *MLL* cDNA probe as described in the legend to Fig. 2. The band induced in apoptotic samples is indicated by an arrow; size standards are in kilobases. (C) Conventional agarose gel electrophoresis of undigested genomic DNA from the experiment described above. Two micrograms of undigested DNA was analyzed per lane. Abbreviations are as indicated above; size standards are in kilobases. (D) The Southern blot shown in panel B, hybridized to a mitochondrial DNA probe. A 17-kb nondegraded band is seen in all lanes and can be contrasted with the partially degraded genomic DNA evident in the apoptotic samples shown in panel C. Abbreviations are as indicated for panel B; size standards are in kilobases.

we were able to detect an oligonucleosomal ladder in cytosine arabinoside-treated MOLT-4 cells (Fig. 3C). The demonstration of an oligonucleosomal ladder did not seem to correlate well with site-specific *MLL* bcr cleavage. Whereas etoposide induced the most dramatic site-specific cleavage, no clear oligonucleosomal ladder could be detected. Also, although cytosine arabinoside and serum starvation produced equivalent evidence of site-specific cleavage (Fig. 3B), an oligonucleosomal ladder is observed in the cytosine arabinoside-treated samples but is absent with serum starvation.

To investigate whether site-specific cleavage was due to a generalized DNA fragmentation process, such as DNA degradation due to necrosis, or due to a more specific, directed DNA cleavage event, we rehybridized the Southern blot shown in Fig. 3B to a mitochondrial DNA probe. In contrast to bulk genomic DNA, mitochondrial DNA has been reported to be resistant to DNA fragmentation induced during apoptosis (58). Although generalized genomic DNA degradation is evident in the apoptotic samples (note the decreased intensity of the 8.3-kb genomic *MLL* fragment in the VP16 and ARA-C lanes in Fig. 3B and the smearing of high-molecular-weight [HMW] DNA in Fig. 3C), the mitochondrial DNA remained intact in the samples which had undergone apoptotic cell death (Fig. 3D). This experiment indicated that although the DNA fragmentation event traditionally associated with apoptotic cell death (oligonucleosomal ladder formation) was not consistently induced, an independent DNA fragmentation event associated with apoptosis (preservation of mitochondrial DNA) was reproducibly present in the samples treated with apoptosis-inducing stimuli. From these experiments, we concluded that site-specific cleavage within the *MLL* bcr resulted from an event which occurred during the process of apoptosis, and although it could be correlated with genomic DNA fragmentation induced by apoptosis, it was distinct

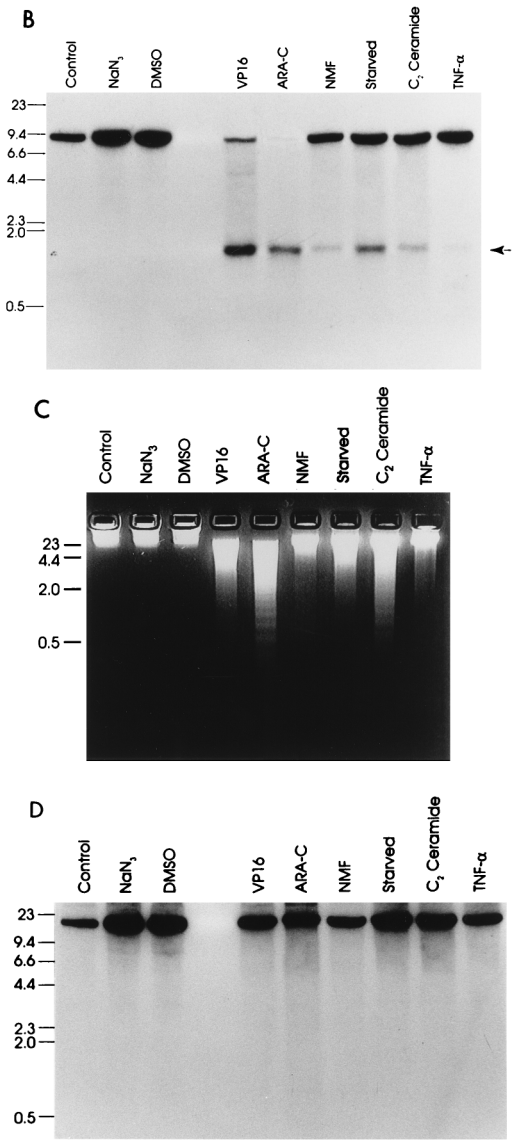

FIG. 3—*Continued.*

from the oligonucleosomal DNA degradation induced by apoptosis.

To determine whether the site-specific cleavage within the *MLL* bcr induced by various apoptotic stimuli was unique to MOLT-4 cells or could be generalized to additional cell lines, we treated the T-cell line CEM with the stimuli used for MOLT-4 cells and obtained a similar induction of site-specific cleavage (Fig. 4A). Differences in the degree of site-specific cleavage induced between MOLT-4 and CEM cells under identical treatment conditions (Fig. 2B, 3B, and 4A) are most likely due to variations in the sensitivity of the two cell lines with respect to the apoptotic stimuli used and correlated with differences in survival fractions estimated by trypan blue exclusion or nuclear fragmentation assays (data not shown). Moreover, site-specific cleavage induced by apoptotic stimuli could be observed in several other cell lines, such as the myeloid leukemia cell lines ML-1 and KG-1, or the solid tumor cell lines 5637 (bladder carcinoma) and H69 (small cell lung cancer) (data not shown). Significantly, we were able to demonstrate site-specific *MLL* cleavage in PBMC from normal donors exposed to either etoposide, *N*-methylformamide, or C_2 ceramide, emphasizing that site-specific *MLL* bcr cleavage during apoptosis is not restricted to malignant cells (Fig. 4B).

Site-specific cleavage within the *MLL* bcr occurs as a part of higher-order chromatin fragmentation during apoptosis. DNA fragmentation during apoptosis is characterized by distinct nuclear events (10). Several groups have studied DNA fragmentation patterns induced by various apoptotic stimuli and concluded that higher-order chromatin fragmentation precedes or occurs simultaneously with the internucleosomal DNA cleavage that generates the characteristic apoptotic ladder (10, 43). Fragments of approximately 50 and/or 300 kb have been observed during the early stages of apoptosis (10, 43); these fragments are thought to represent cleavage of higher-order chromatin structures, such as looped chromosomal DNA. In many but not all cell types, this HMW DNA fragmentation is followed by subsequent cleavage of DNA to oligonucleosome-size integers of multiples of about 180 bp, which are responsible for the typical DNA ladder associated with apoptosis (10, 43).

Since *MLL* site-specific cleavage seemed to be associated with DNA degradation during apoptosis but not consistently with oligonucleosomal ladder formation, we investigated the possibility that site-specific cleavage was associated with a DNA fragmentation event during apoptosis which was distinct from oligonucleosomal cleavage. More specifically, we wished to determine whether the site-specific cleavage within the *MLL* bcr could be linked to one of the discrete steps described for higher-order chromatin fragmentation during apoptosis induced by topo II inhibitors (7). Therefore, we treated MOLT-4 cells with 30 μM etoposide for 6 h, embedded the cells in agarose plugs, size fractionated HMW genomic DNA by FIGE, and gel purified the 40- to 60-kb fraction. This fraction showed site-specific *MLL* cleavage when analyzed by indirect end labeling using the 0.7B and 0.2HB *MLL* cDNA probes (data not shown). The finding that *MLL* site-specific cleavage occurs within the 40- to 60-kb fraction is consistent with the possibility that apoptosis induces DNA cleavage specifically at the SAR previously mapped within the *MLL* bcr (57).

Site-specific cleavage within the *MLL* bcr is conserved between species. Since site-specific cleavage within the *MLL* bcr had been mapped to a high-affinity SAR (57), and SARs appear to be evolutionarily conserved (15, 16, 54), we investigated the possibility that site-specific cleavage within the *MLL* bcr induced by apoptosis is conserved between species. To

TABLE 1. Cell viability and apoptosis of MOLT-4 cells in response to necrotic and apoptotic stimuli[a]

Stimulus	Trypan blue exclusion (%)	Nuclear fragmentation (%)
Control	100	0
300 mM sodium azide	0	0
30% DMSO	0	0
30 μM etoposide	16	87
3 μg of cytosine arabinoside/ml	38	71
300 mM *N*-methylformamide	60	52
25 μM C_2 ceramide	67	51
Serum starvation (56 h)	48	64
10 nM TNF-α	91	15

[a] Cell viability was assessed by trypan blue exclusion; apoptosis was assessed by nuclear fragmentation with Hoechst 33258 staining as described in Materials and Methods. The results represent the mean values obtained from three experiments.

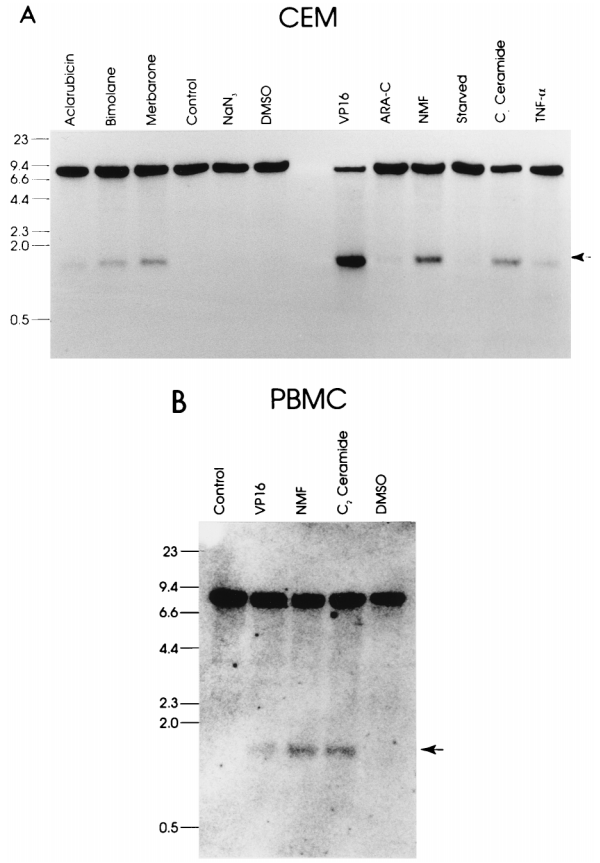

FIG. 4. (A) Site-specific cleavage within the *MLL* bcr is induced by apoptosis in CEM cells. Cells were either treated for 16 h with 0.1 μM aclarubicin, 20 μM bimolane, 10 μM merbarone, vehicle alone (Control; 0.03% DMSO), 300 mM sodium azide (NaN_3), 30% DMSO, 30 μM etoposide (VP16), 3 μg of cytosine arabinoside (ARA-C) per ml, 300 mM *N*-methylformamide (NMF), 25 μM C_2 ceramide, and 10 nM TNF-α or subjected to 56 h of serum withdrawal (Starved). Genomic DNA was analyzed by indirect end labeling using the 0.2HB *MLL* cDNA probe. The band induced in the apoptotic samples is indicated by an arrow; size standards are in kilobases. (B) Site-specific cleavage within the *MLL* bcr is detected in PBMC of a normal individual. Treatment conditions and abbreviations are as described above. The treatment-induced band is indicated by an arrow; size standards are in kilobases.

assess this possibility, we treated the murine leukemia cell lines LBRM-33 and F4-6 with etoposide, *N*-methylformamide, and C_2 ceramide to induce apoptosis. The mode of cell death was analyzed by the nuclear fragmentation assay, using the DNA-specific fluorochrome Hoechst 33258. Genomic DNA from these experiments was analyzed by indirect end labeling with the human 0.2HB *MLL* cDNA probe, which contains exons 9 to 11 and shows 91% sequence identity with its murine counterpart in this region. Figure 5 demonstrates site-specific cleavage of the murine *MLL* in LBRM-33 cells treated with etoposide and assayed by indirect end labeling. Site-specific cleavage was also inducible by *N*-methylformamide and C_2 ceramide (data not shown).

Site-specific cleavage within the *AML1* bcr is also inducible by apoptosis. Translocations involving the *AML1* locus on chromosome 21q22 not only are observed in de novo AML but also are commonly recognized in t-AML associated with topo II inhibitor treatment (44, 45). Although we had previously been unable to detect site-specific cleavage inducible by topo II inhibitors at several loci frequently disrupted by chromosomal translocations, including *SCL/TAL*, *ENL*, *AF-6*, c-*myc*, and the T-cell receptor β and δ chains (5), we have recently identified site-specific cleavage inducible by topo II inhibitors at a unique site within the *AML1* bcr (56). This finding demonstrated that site-specific cleavage inducible by topo II inhibitors was not solely restricted to the *MLL* bcr. In contrast to *MLL* site-specific cleavage, which is clearly detectable in both malignant cell lines and PBMC, *AML1* cleavage was only faintly visible in PBMC of healthy normal individuals, suggesting that the *MLL* site is more sensitive to site-specific cleavage. To investigate whether site-specific cleavage within the *AML1* bcr is also linked to apoptosis, we rehybridized the Southern blots shown in Fig. 3B and 4A to the C6E6H2 *AML1* cDNA probe containing *AML1* exons 5 and 6 (39) (Fig. 6A). Here, site-specific cleavage within the *AML1* locus between exons 5 and 6 was detectable in DNA isolated from MOLT-4 (Fig. 6B) and CEM (data not shown) cells that were treated with apoptosis-inducing stimuli but not in DNA isolated from cells undergoing necrotic cell death. Thus, we provide evidence that site-specific genomic DNA cleavage during apoptosis occurs not only within the *MLL* bcr but also within the *AML1* bcr.

DISCUSSION

Over the past several years, t-AML following chemotherapy with agents targeting topo II has been recognized with increasing frequency. t-AML associated with antecedent topo II inhibitor treatment displays distinct cytogenetic features, most often translocations of the *MLL* gene on chromosome 11q23 and, to a lesser extent, the *AML1* gene on chromosome 21q22 (44, 45, 48, 53). Since topo II inhibitors are among the most

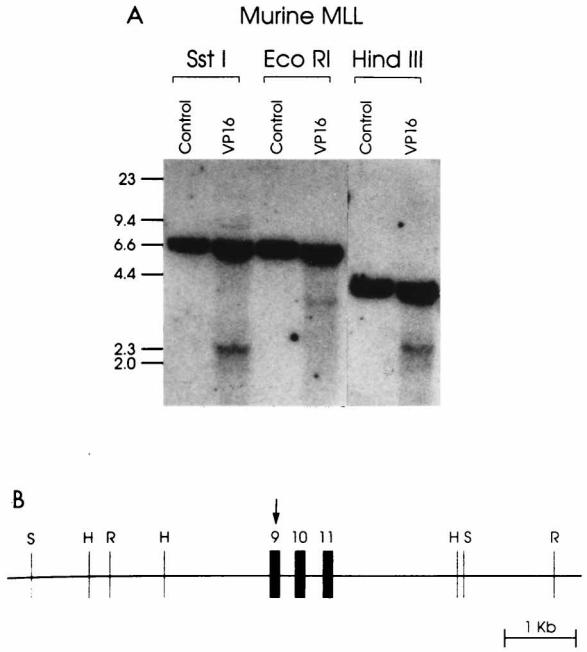

FIG. 5. (A) Site-specific cleavage within the murine *MLL* locus. LRBM-33 cells were treated for 16 h with vehicle alone (Control; 0.01% DMSO) or 10 μM etoposide (VP16). Genomic DNA was digested with the indicated restriction enzyme, size fractionated, transferred to nitrocellulose, and analyzed by indirect end labeling to the human 0.2HB *MLL* cDNA probe. Etoposide-induced bands are evident in the VP16-treated lanes. Size standards are in kilobases. (B) Restriction map of the relevant region of the murine *MLL* locus. Exons 9, 10, and 11 were assigned based on ≈90% nucleotide sequence identity with the human *MLL*; exon/intron junctions were sequenced to verify the splice sites. Indicated restriction enzyme sites: R, *Eco*RI; S, *Sst*I; H, *Hin*dIII. The point of site-specific cleavage is indicated by an arrow.

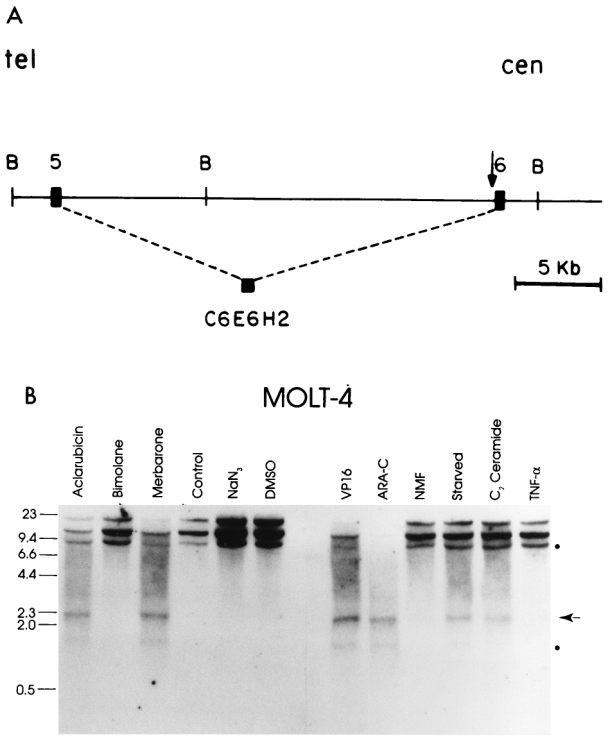

FIG. 6. (A) Partial restriction map of *AML1*, as previously reported (39). Chromosomal orientation from centromere (cen) to telomere (tel) is as indicated. Exons are shown as solid boxes, the previously identified cleavage site induced by etoposide treatment is indicated by an arrow, and the cDNA probe C6E6H2, containing *AML1* exon 5 and 6 sequences, is indicated. Restriction sites for *Bam*HI (B) are indicated. (B) Site-specific cleavage within the *AML1* bcr induced by various apoptotic stimuli but not by necrotic stimuli. MOLT-4 cells were treated for 16 h as described in the legend to Fig. 4A and hybridized to the C6E6H2 probe. Germ line bands are seen at 20 and 11 kb, a treatment-induced band is indicated with an arrow, and residual *MLL* hybridization signals are shown with closed circles.

useful cancer chemotherapeutic agents, elucidating the events which lead to these translocations is of both clinical and biological interest. In this report, we demonstrate that site-specific DNA double-strand cleavage at a unique site within the *MLL* bcr can be generated in response to various apoptotic stimuli. The proportion of cells demonstrating site-specific *MLL* cleavage varied with different apoptotic stimuli as well as between cell lines, which most likely reflected different sensitivities of the cell lines to the different apoptotic stimuli used. Site-specific *MLL* bcr cleavage was generalizable from malignant cells to PBMC of healthy normal individuals and could be linked to the higher-order chromatin fragmentation which occurs during the early stages of apoptosis. In addition, site-specific cleavage within the *MLL* bcr seems to be conserved between species, since it can be induced in both the human and murine *MLL* loci. Lastly, site-specific double-strand DNA cleavage induced by apoptosis could be extended to the *AML1* locus.

DNA cleavage produced in vitro by using purified topo II and topo II inhibitors does not always correlate well with DNA cleavage induced by topo II inhibitors in vivo. For instance, analysis of the *Drosophila* histone repeat locus has demonstrated that cleavage sites induced by topo II inhibitors in vivo were only weakly induced in vitro (30). These findings suggest that variables such as chromatin structure and accessibility are likely to be important factors influencing preferred DNA cleavage sites induced by topo II inhibitors in intact cells. Our in vitro experiments performed with a cloned genomic fragment encompassing the *MLL* bcr mapped one of the most prominent cleavage sites induced by the topo II inhibitor etoposide to the same region as cleavage induced by topo II inhibitor treatment of intact cells. This is not surprising, given that the only perfect in vitro topo II consensus sequence (55) within the *MLL* bcr also maps to this region (5). However, this experiment does not prove that topo II-cleavable complex formation is directly involved in the site-specific *MLL* cleavage that occurs in intact cells; an alternate interpretation may be that apoptotic stimuli (including topo II inhibitors) generate higher-order chromatin fragmentation beginning with cleavage at chromosomal loop attachment regions (SARs), where topo II has been localized as a structural chromatin element.

Topo II is likely to be an important structural element of the nuclear scaffold, as it can be localized to the base of chromatin loops (19) and has been shown to bind SAR sequences, which are the proposed anchorage regions of DNA loops to the nuclear scaffold (1, 38, 54). A recently described technique (28, 49) that employs histone-depleted nuclei has been used to colocalize previously mapped SARs with topo II inhibitor-induced cleavage sites on the *Drosophila* X chromosome (28), providing support for the model that the DNA fragments generated by topo II inhibitor treatment of nuclei represent DNA loops excised from the nuclear scaffold via topo II-mediated cleavage at their SARs.

As mentioned above, the initial DNA fragmentation event associated with apoptosis, generally preceding oligonucleosomal ladder formation, seems to be cleavage of DNA into large (50- to 300-kb) fragments (10, 43), close to the estimated average size (86 kb) of a chromosomal loop (29). This observation has led to the suggestion that apoptotic degradation of chromosomal DNA starts by excision of DNA loops from their anchorage regions on the nuclear scaffold (10, 43). Experimental support for this model has come from a report which demonstrates that the pattern of DNA fragmentation produced by apoptosis is identical to the pattern of DNA fragmentation obtained by cleavage at loop anchorage sites using the topo II inhibitor-mediated DNA loop excision protocol (33).

A high-affinity SAR has been mapped to the telomeric portion of the *MLL* bcr near *MLL* exon 9 (57); we have previously shown that site-specific cleavage within the *MLL* bcr also maps to *MLL* exon 9 (5) and therefore colocalizes with the above-described SAR. These observations lead us to suspect that site-specific *MLL* cleavage which occurs in response to apoptotic stimuli may reflect cleavage at an SAR within the telomeric portion of the *MLL* bcr. Whether this cleavage is mediated either by an endonuclease associated with apoptosis or by a direct enzymatic effect of topo II remains unclear. Also, it is unclear if the specific cleavage identified within the *MLL* bcr reflects a SAR with unusual sensitivity to the higher-order chromatin fragmentation that occurs in response to apoptotic stimuli; it is possible that SARs displaying a similar degree of specific cleavage exist throughout the genome. However, the only other single-copy locus that we have identified thus far that displays a similar degree of inducible site-specific cleavage is the *AML1* locus (56), which, like *MLL*, is associated with chromosomal translocations induced by multiagent chemotherapy regimens including topo II inhibitors.

Previous investigations of genomic DNA cleavage induced by apoptosis have generally studied either oligonucleosomal cleavage (10, 61, 63), bulk genomic DNA (43), or amplified or repeat loci (33). Some of these studies have used pulsed-field gel electrophoresis or FIGE to examine long-range fragmentation; the resolving ability of those gels limited localization of cleavage sites to regions of approximately 5 kb (28). This re-

port has demonstrated the feasibility of studying DNA fragmentation induced by apoptosis at the level of a single-copy locus within a complex mammalian genome and demonstrated that this fragmentation can be localized to very specific regions (estimated to be a maximum of 100 bp) within genomic DNA.

The data presented here lead to a potential mechanism for chromosomal rearrangements, including translocations, that involves the higher-order chromatin fragmentation that occurs during apoptosis. A stimulus, such as a cancer chemotherapeutic agent, induces apoptosis in a target cell population, leading to the initiation of higher-order chromatin fragmentation through excision of DNA loops at their anchorage sites from the nuclear scaffold, mediated by either topo II or an apoptotic endonuclease. Although initiation of apoptosis in the vast majority of cells leads to a cell death commitment, upon removal of the apoptotic stimulus, a rare population of cells may not complete the apoptosis program but rather attempt to reverse the apoptotic process. Upon this reversal, the DNA damage caused by loop cleavage is repaired by religation of the cleaved loops. Some of these cells repair their damage incorrectly, leading to chromosomal rearrangements including translocations. The telomeric portion of the *MLL* bcr is a preferred target for specific cleavage resulting from higher-order chromatin fragmentation during apoptosis and therefore would be a preferred target region for chromosomal translocations caused by this mechanism. Of note, there are several reports of patients with t-AML characteristic of t-AML associated with topo II inhibitor therapy (a short latency period, monocytic phenotype, and *MLL* translocations) whose chemotherapeutic regimens did not incorporate topo II inhibitors but who were instead treated with chemotherapeutic drugs such as alkylating agents or antimetabolites (20, 32, 46), which can induce apoptosis. While these t-AML cases may in fact be de novo leukemias, an alternate explanation would be that a chemotherapeutic agent which does not target topo II, but which can induce apoptosis, had caused the translocation. With this speculative model in mind, it is interesting that overexpression of *bcl2* has been shown to decrease sister chromatid exchange and other rearrangements induced by etoposide while not affecting cleavable complex formation induced by etoposide (25).

The *MLL* breakpoints recognized in t-AML patients seem to cluster within a region approximately 2 kb centromeric to the specific cleavage site identified within exon 9 (57) rather than precisely at the exon 9 cleavage site. One potential explanation for this observation is that the double-strand DNA cleavage which occurs at the exon 9 site may be followed by a variable amount of exonucleolytic DNA degradation and subsequent religation to a different chromosome, producing a translocation. If this model is correct, the *MLL* translocations which occur in t-AML should have small regions centromeric to *MLL* exon 9 that are deleted. Verification of this model is dependent on cloning and sequencing the relevant derivative translocated chromosomes from t-AML patients.

In conclusion, our study demonstrates that the *MLL* and *AML1* loci are specifically cleaved at unique sites within their bcrs during the early stages of apoptosis. The observed cleavage is independent of the stimuli used to induce apoptosis, is conserved between species, can be localized to a narrow (<100-bp) region, and seems to be independent of the catalytic activity of topo II. In addition, this report demonstrates the feasibility of studying the effect of DNA fragmentation which occurs during apoptosis at the level of single-copy loci within complex mammalian genomes. Lastly, the fact that the two cleavage sites identified are within bcrs mapped in patients with t-AML suggests a link between the higher-order DNA fragmentation which occurs during apoptosis and chromosomal translocations induced by genotoxic cancer chemotherapeutic agents.

ACKNOWLEDGMENTS

This work was supported in part by grants from the Roswell Park Alliance Foundation, the Association for the Research of Childhood Cancer, and the NIH (grant CA16056-21) (P.D.A.) and from the Deutsche Forschungsgemeinschaft (M.S.). P.D.A. is a Scholar of the Leukemia Society of America.

REFERENCES

1. **Adachi, Y., E. Käs, and U. K. Laemmli.** 1989. Preferential, cooperative binding of DNA topoisomerase II to scaffold-associated regions. EMBO J. **8:**3997–4006.
2. **Adams, J. M., and S. Cory.** 1991. Transgenic models of tumor development. Science **254:**1161–1167.
3. **Aplan, P. D., C. G. Begley, V. L. Bertness, M. Nussmeier, A. Ezquerra, J. Coligan, and I. R. Kirsch.** 1990. The *SCL* gene is formed from a transcriptionally complex locus. Mol. Cell. Biol. **10:**6426–6435.
4. **Aplan, P. D., D. P. Lombardi, A. M. Ginsberg, J. Cossman, V. L. Bertness, and I. R. Kirsch.** 1990. Disruption of the human *SCL* locus by "illegitimate" V(D)J recombinase activity. Science **250:**1426–1429.
5. **Aplan, P. D., D. S. Chervinsky, M. Stanulla, and W. C. Burhans.** 1996. Site-specific DNA cleavage within the *MLL* breakpoint cluster region induced by topoisomerase II inhibitors. Blood **87:**2649–2658.
6. **Beck, W. T., and M. K. Danks.** 1991. Mechanisms of resistance to drugs that inhibit DNA topoisomerases. Semin. Cancer Biol. **2:**235–244.
7. **Beere, H. M., C. M. Chresta, A. Alejo-Herberg, A. Skladanowski, C. Dive, A. Kragh Larsen, and J. A. Hickman.** 1995. Investigation of the mechanism of higher order chromatin fragmentation observed in drug-induced apoptosis. Mol. Pharmacol. **47:**986–996.
8. **Berezney, R., and D. S. Coffey.** 1974. Identification of a nuclear protein matrix. Biochem. Biophys. Res. Commun. **60:**1410–1419.
9. **Bishop, J. M.** 1995. The rise of the genetic paradigm. Genes Dev. **9:**1309–1315.
10. **Bortner, C. D., N. B. E. Oldenburg, and J. A. Cidlowski.** 1995. The role of DNA fragmentation in apoptosis. Trends Cell Biol. **5:**21–26.
11. **Catchpoole, D. R., and B. W. Stewart.** 1993. Etoposide-induced cytotoxicity in two human T-cell leukemic lines: delayed loss of membrane permeability rather than DNA fragmentation as an indicator of programmed cell death. Cancer Res. **53:**4287–4296.
12. **Chen, M., and W. T. Beck.** 1993. Teniposide-resistant CEM cells, which express mutant DNA topoisomerase IIa, when treated with non-complex-stabilizing inhibitors of the enzyme, display no cross-resistance and reveal aberrant functions of the mutant enzyme. Cancer Res. **53:**5946–5953.
13. **Cifone, M. G., R. DeMaria, P. Roncaioli, M. R. Rippo, M. Azuma, L. L. Lanier, A. Santoni, and R. Testi.** 1994. Apoptotic signaling through CD95 (Fas/Apo-1) activates an acidic sphingomyelinase. J. Exp. Med. **177:**1547–1552.
14. **Cline, M. J.** 1994. The molecular basis of leukemia. N. Engl. J. Med. **330:**328–336.
15. **Cockerill, P. N., and W. T. Garrard.** 1986. Chromosomal loop anchorage of the kappa immunoglobulin gene occurs next to the enhancer in a region containing topoisomerase II sites. Cell **44:**273–282.
16. **Cockerill, P. N., and W. T. Garrard.** 1986. Chromosomal loop anchorage sites appear to be evolutionary conserved. FEBS Lett. **204:**5–7.
17. **Danks, M. K., C. A. Schmidt, M. L. Cirtain, D. P. Suttle, and W. T. Beck.** 1988. Altered catalytic activity of and DNA cleavage by DNA topoisomerase II from human leukemic cells selected for resistance to VM-26. Biochemistry **27:**8861–8869.
18. **Davis, L. G., M. D. Dibner, and J. F. Battey.** 1986. Basic methods in molecular biology. Elsevier, New York, N.Y.
19. **Earnshaw, W. C., B. Halligan, C. A. Cooke, M. S. Heck, and L. F. Liu.** 1986. Topoisomerase II is a structural component of mitotic chromosome scaffolds. J. Cell Biol. **100:**1706–1715.
20. **Felix, C. A., M. R. Hosler, N. J. Winick, M. E. Masterson, A. E. Wilson, and B. J. Lange.** 1995. *ALL-1* gene rearrangements in DNA topoisomerase II inhibitor-related leukemia in children. Blood **85:**3250–3256.
21. **Fernandes, D. J., M. K. Danks, and W. T. Beck.** 1990. Decreased nuclear matrix DNA topoisomerase II in human leukemia cells resistant to VM-26 and m-AMSA. Biochemistry **29:**4235–4241.
22. **Fisher, D. E.** 1994. Apoptosis in cancer therapy: crossing the threshold. Cell **78:**539–542.
23. **Gasser, S. M., and U. K. Laemmli.** 1986. Cohabitation of scaffold binding regions with upstream/enhancer elements of three developmentally regulated genes of D. melanogaster. Cell **46:**521–530.
24. **Gill-Super, H. J., N. R. McCabe, M. J. Thirman, R. A. Larson, M. M. LeBeau, J. Pedersen-Bjergaard, P. Preben, M. Diaz, and J. D. Rowley.** 1993. Rearrangements of the *MLL* gene in therapy-related acute myeloid leuke-

mia in patients previously treated with agents targeting DNA topoisomerase II. Blood **82:**3705–3711.
25. **Hashimoto, H., S. Chatterjee, and N. A. Berger.** 1995. Inhibition of etoposide (VP-16)-induced DNA recombination and mutant frequency by Bcl-2 protein overexpression. Cancer Res. **55:**4029–4035.
26. **Hickman, J. A.** 1992. Apoptosis induced by anticancer drugs. Cancer Metastasis Rev. **11:**121–139.
27. **Houge, G., B. Robaye, T. S. Eikhom, J. Golstein, G. Mellgren, B. T. Gjertsen, M. Lanotte, and S. O. Døskeland.** 1995. Fine mapping of 28S rRNA sites specifically cleaved in cells undergoing apoptosis. Mol. Cell. Biol. **15:**2051–2062.
28. **Iarovaia, O., R. Hancock, M. Lagarkova, R. Miassod, and S. V. Razin.** 1996. Mapping of genomic DNA loop organization in a 500-kilobase region of the *Drosophila* X chromosome by the topoisomerase II-mediated DNA loop excision protocol. Mol. Cell. Biol. **16:**302–308.
29. **Jackson, D. A., P. Dickinson, and P. R. Cook.** 1990. The size of chromatin loops in HeLa cells. EMBO J. **9:**567–571.
30. **Kas, E., and U. K. Laemmli.** 1992. In vivo topoisomerase II cleavage of the Drosophila histone and satellite III repeats: DNA sequence and structural characteristics. EMBO J. **11:**705–716.
31. **Kaufmann, H.** 1989. Induction of endonucleolytic DNA cleavage in human acute myelogenous leukemia cells by etoposide, camphotecin and other cytotoxic anticancer drugs: a cautionary note. Cancer Res. **49:**5870–5878.
32. **Kubota, M., Y. Hoshino, H. Doi, H. Ueno, Y. Nishida, H. Hirota, and Y. Akiyama.** 1994. Myelodysplastic syndrome with t(9;11)(p22;q23) after treatment for B-cell acute lymphoblastic leukemia without epipodophyllotoxins. Acta Haematol. **92:**33–35.
33. **Lagarkova, M. A., O. V. Iarovaia, and S. V. Razin.** 1996. Large-scale fragmentation of mammalian DNA in the course of apoptosis proceeds via excision of chromosomal DNA loops and their oligomers. J. Biol. Chem. **270:**20239–20241.
34. **Laster, S. M., J. G. Wood, and L. R. Gooding.** 1988. Tumor necrosis factor can induce both apoptotic and necrotic forms of cell lysis. J. Immunol. **141:**2629–2635.
35. **Mamuris, Z., M. Prieur, B. Dutrillaux, and A. Aurias.** 1989. The chemotherapeutic drug melphalan induces breakage of chromosome regions rearranged in secondary leukemia. Cancer Genet. Cytogenet. **37:**65–77.
36. **Maraschin, J., B. Dutrillaux, and A. Aurias.** 1990. Chromosome aberrations induced by etoposide (VP-16) are not random. Int. J. Cancer **46:**808–812.
37. **McCabe, N. R., R. C. Burnett, H. J. Gill, M. J. Thirmann, D. Mbangkollo, M. Kipiniak, E. van Melle, S. Ziemin-van der Poel, J. D. Rowley, and M. O. Diaz.** 1992. Cloning of cDNAs of the *MLL* gene that detect DNA rearrangements and altered RNA transcripts in human leukemic cells with 11q23 translocations. Proc. Natl. Acad. Sci. USA **89:**11794–11799.
38. **Mircovich, J., M. E. Mirault, and U. K. Laemmli.** 1984. Organization of the higher-order chromatin loop: specific DNA attachment sites on nuclear scaffold. Cell **39:**223–232.
39. **Miyoshi, H., K. Shimizu, T. Kozu, N. Maseki, Y. Kaneko, and M. Ohki.** 1991. t(8;21) breakpoints on chromosome 21 in acute myeloid leukemia are clustered within a limited region of a single gene, *AML1*. Proc. Natl. Acad. Sci. USA **88:**10431–10434.
40. **Morganbesser, S. D., and R. A. DePinho.** 1994. Use of transgenic mice to study myc family gene function in normal mammalian development and in cancer. Semin. Cancer Biol. **5:**21–36.
41. **Nedospasov, S. A., and G. P. Georgiev.** 1980. Non-random cleavage of SV40 DNA in the compact minichromosome and free in solution by micrococcal nuclease. Biochem. Biophys. Res. Commun. **92:**532–539.
42. **Oberhammer, F. A., M. Pavelka, S. Sharma, R. Tiefenbacher, A. F. Purchio, W. Bursch, and R. Schulte-Hermann.** 1992. Induction of apoptosis in cultured hepatocytes and in regressing liver by transforming growth factor β1. Proc. Natl. Acad. Sci. USA **89:**5408–5412.
43. **Oberhammer, F. A., J. W. Wilson, C. Dive, I. D. Morris, J. A. Hickman, A. E. Wakeling, P. R. Walker, and M. Sikorska.** 1993. Apoptotic death in epithelial cells: cleavage of DNA to 300 and/or 50 kb fragments prior to or in absence of internucleosomal fragmentation. EMBO J. **12:**3679–3684.
44. **Pedersen-Bjergaard, J., and P. Philip.** 1991. Balanced translocations involving chromosome bands 11q23 and 21q22 are highly characteristic of myelodysplasia and leukemia following therapy with cytostatic agents targeting a topoisomerase II. Blood **78:**1147–1148.
45. **Pedersen-Bjergaard, J., M. Pedersen, D. Roulsten, and P. Philip.** 1995. Different genetic pathways in leukemogenesis for patients presenting with therapy-related myelodysplasia and therapy-related acute myeloid leukemia. Blood **86:**3542–3552.
46. **Philpott, N. J., M. O. Elebute, R. Powles, J. G. Treleaven, M. Gore, M. G. Dainton, T. Min, G. J. Swansbury, and D. Catovsky.** 1996. Platinum agents and secondary leukemia: two cases treated only with platinum-based drugs. Br. J. Haematol. **93:**884–887.
47. **Rabbitts, T. H.** 1994. Chromosomal translocations in human cancer. Nature **372:**143–149.
48. **Ratain, M. J., L. S. Kaminer, J. D. Bitran, R. A. Larson, M. M. LeBeau, C. Shosey, S. Purl, P. C. Hofman, J. Wade, J. W. Vardiman, K. Daly, J. D. Rowley, and H. M. Golomb.** 1987. Acute nonlymphocytic leukemia following etoposide and cisplatin combination therapy for advanced small-cell carcinoma of the lung. Blood **70:**1412–1417.
49. **Razin, S. V., P. Petrov, and R. Hancock.** 1991. Precise localization of the α-globin cluster within one of the 20- to 300-kilobase DNA fragments released by cleavage of chicken chromosomal DNA at topoisomerase II sites in vivo: evidence that the fragments are DNA loops or domains. Proc. Natl. Acad. Sci. USA **88:**8515–8519.
50. **Rubnitz, J. E., F. G. Behm, and J. R. Downing.** 1996. 11q23 rearrangements in acute leukemia. Leukemia **10:**74–82.
51. **Sambrook, J., E. F. Fritsch, and T. Maniatis.** 1989. Molecular cloning: a laboratory manual. Cold Spring Harbor Laboratory Press, Cold Spring Harbor, N.Y.
52. **Schichman, S. A., M. A. Caligiuri, M. P. Strout, S. L. Carter, Y. Gu, E. Canaani, C. D. Bloomfield, and C. M. Croce.** 1994. *ALL-1* tandem duplication in acute myeloid leukemia with normal karyotype involves homologous recombination between Alu elements. Cancer Res. **54:**4277–4280.
53. **Smith, M. A., R. P. McCaffrey, and J. E. Karp.** 1996. The secondary leukemias: challenges and research directions. J. Natl. Cancer Inst. **88:**407–418.
54. **Sperry, A. O., V. C. Blasquez, and W. T. Garrard.** 1989. Dysfunction of chromosomal loop attachment sites: illegitimate recombination linked to matrix association regions and topoisomerase II. Proc. Natl. Acad. Sci. USA **86:**5497–5501.
55. **Spitzner, J. R., and M. T. Muller.** 1988. A consensus sequence for cleavage by vertebrate DNA topoisomerase II. Nucleic Acids Res. **16:**5533–5556.
56. **Stanulla, M., J. J. Wang, D. Chervinsky, and P. D. Aplan.** 1997 Topoisomerase II inhibitors induce DNA double strand breaks at a specific site within the *AML1* locus. Leukemia **11:**490–496.
57. **Strissel Broeker, P. L., H. Gill Super, M. J. Thirman, H. Pomykala, Y. Yonebashi, S. Tanabe, N. Zeleznik-Le, and J. D. Rowley.** 1996. Distribution of 11q23 breakpoints within the MLL breakpoint cluster region in de novo acute myeloid leukemia and in treatment-related acute myeloid leukemia: correlation with scaffold attachment regions and topoisomerase II binding sites. Blood **87:**1912–1922.
58. **Tepper, C. G., and G. P. Studzinski.** 1993. Resistance of mitochondrial DNA to degradation characterizes the apoptotic but not the necrotic mode of human leukemia cell death. J. Cell. Biochem. **52:**352–361.
59. **Thirman, M. J., H. J. Gill, R. C. Burnett, D. Mbangkollo, N. R. McCabe, H. Kobayashi, S. Ziemin-van der Poel, Y. Kaneko, R. Morgan, A. A. Sandberg, R. S. K. Chaganti, R. A. Larson, M. M. LeBeau, M. O. Diaz, and J. D. Rowley.** 1993. Rearrangement of the *MLL* gene in acute lymphoblastic and acute myeloid leukemias with 11q23 chromosomal translocations. N. Engl. J. Med. **329:**909–914.
60. **Tycko, B., and J. Sklar.** 1990. Chromosomal translocations in lymphoid neoplasia: a reappraisal of the recombinase model. Cancer Cells **2:**1–8.
61. **White, E.** 1993. Death-defying acts: a meeting review on apoptosis. Genes Dev. **7:**2277–2284.
62. **Winick, N. J., R. W. McKenna, J. J. Shuster, N. R. Schneider, M. J. Borowitz, W. P. Bowman, D. Jacaruso, B. A. Kamen, and G. R. Buchanan.** 1993. Secondary acute myeloid leukemia in children with acute lymphoblastic leukemia treated with etoposide. J. Clin. Oncol. **11:**209–217.
63. **Wyllie, A. H., J. F. R. Kerr, and A. R. Currie.** 1980. Cell death: the significance of apoptosis. Int. Rev. Cytol. **68:**251–306.